

Moiré Patterns in a bilayer: electronic structure

J.M.B. Lopes dos Santos

CFP and Departamento de Física, Universidade do Porto

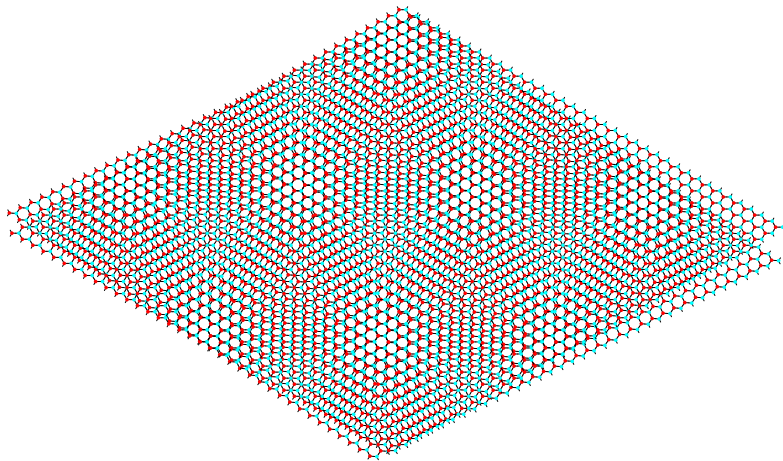
Graphene Workshop, KITP, January, 2007

- Nuno Peres (U. Minho)
- Antonio Castro Neto (Boston U)
- Vítor Pereira (U. Porto and Boston U.)

Acknowledgments: FCT

What is a Moiré pattern?

A beat between periods



Moiré in graphite

Electronic effects in scanning tunneling microscopy: Moiré pattern on a graphite surface

Zhao Y. Rong and Pieter Kuiper

Physics Department, Brookhaven National Laboratory, Upton, New York 11973

Received 27 July 1993

We observed by scanning tunneling microscopy (STM) a hexagonal superlattice on graphite with a period of 66 Å. Direct measurement of the angle between lattice vectors confirmed that the superlattice is a Moiré pattern caused by a 2.1° rotation of the topmost (0001) plane with respect to the bulk. The STM corrugation of 2.6 Å is not due to physical buckling, but to differences in electronic structure between *AA*-stacked, normal *AB*-stacked, and rhombohedral *CAB*-stacked graphite. The high tunneling current of *AA*-stacked regions is in agreement with the high density of states at the Fermi level calculated for *AA* graphite. The Moiré pattern changes, both the amplitude and the shape, with bias voltage. The observation provides a basis for a comparative study of surface electronic structures with different subsurface layer configuration, which is a vital test of our understanding of STM.

©1993 The American Physical Society

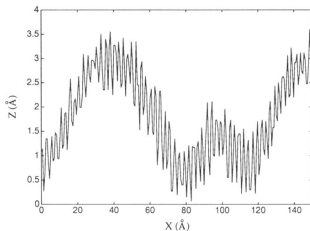
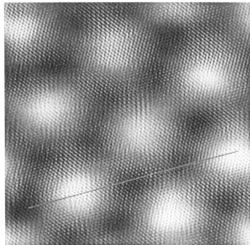
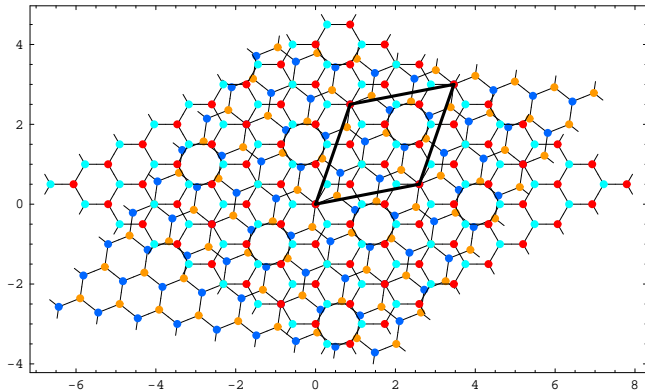


FIG. 2. (a) A closeup view of the superlattice on which graphite atoms are resolved. The image is taken with set current 5.6 nA, tip bias 72 mV, and scan size $202 \times 202 \text{ \AA}^2$. The image is low pass filtered. (b) A cross section along the direction indicated by the line in (a).

Rong and Kuiper, PRB 1993

- Commensurability conditions
- Continuum modeling: quasi-free Dirac fermions
- Calculation of inter-layer hopping
- Electronic structure.

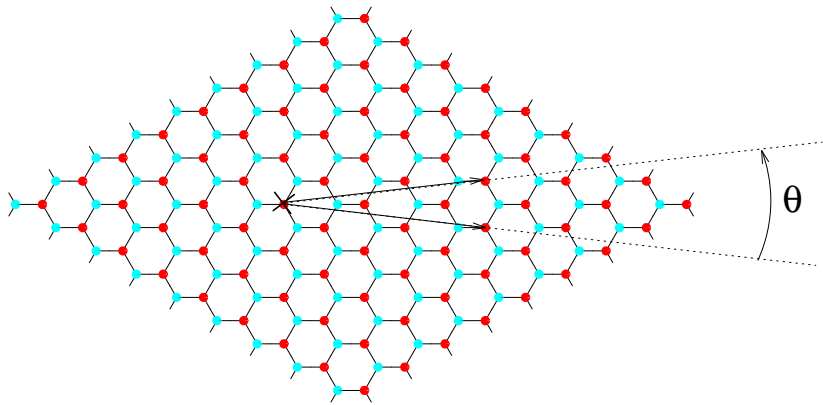
Commensurability angles



$$\cos(\theta_i) = \frac{1 + 1/i + 1/(6i^2)}{1 + 1/i + 1/(3i^2)} \quad (1)$$

$$i = 15 \Rightarrow \theta = 2.13^\circ, \quad L = 66 \text{ \AA}$$

Superlattice basis



$$\begin{aligned} \mathbf{t}_1 &= (i+1)\mathbf{a}_1 + i\mathbf{a}_2 \\ \mathbf{t}_2 &= (2i+1)\mathbf{a}_1 - (i+1)\mathbf{a}_2. \end{aligned} \quad (2)$$

Continuum modeling

- Single Layer

$$\mathcal{H}_1 = -t \sum_i a_1^\dagger(\mathbf{r}_i) [b_1(\mathbf{r}_i - \mathbf{s}_0) + b_1(\mathbf{r}_i - \mathbf{s}_0 + \mathbf{a}_1) + b_1(\mathbf{r}_i - \mathbf{s}_0 + \mathbf{a}_2)] + hc$$

$$\begin{aligned} a_1(\mathbf{r}) &\rightarrow v_c^{1/2} \psi_a(\mathbf{r}) \exp(i\mathbf{K} \cdot \mathbf{r}) \\ b_1(\mathbf{r}) &\rightarrow v_c^{1/2} \psi_b(\mathbf{r}) \exp(i\mathbf{K} \cdot \mathbf{r}) \end{aligned}$$

$$\hbar v_F \sum_{\mathbf{k}} \psi'^{\dagger}(\mathbf{k}) \begin{bmatrix} 0 & (k_x - ik_y) \\ (k_x + ik_y) & 0 \end{bmatrix} \psi'(\mathbf{k}).$$

Continuum Modeling

- Rotated Layer

$$\mathcal{H}_2 = -t \sum_j b_2^\dagger(\mathbf{r}_j) [a_2(\mathbf{r}_j + \mathbf{s}'_0) + a_2(\mathbf{r}_j + \mathbf{s}'_0 - \mathbf{a}'_1) + a_2(\mathbf{r}_j + \mathbf{s}'_0 - \mathbf{a}'_2)] + h.c.$$

$$\begin{aligned} a_2(\mathbf{r}) &\rightarrow v_c^{1/2} \psi_{a'}(\mathbf{r}) \exp(i\mathbf{K}^\theta \cdot \mathbf{r}) \\ b_2(\mathbf{r}) &\rightarrow v_c^{1/2} \psi_{b'}(\mathbf{r}) \exp(i\mathbf{K}^\theta \cdot \mathbf{r}) \end{aligned}$$

$$\hbar v_F \sum_k \psi'^\dagger(\mathbf{k}) \begin{bmatrix} 0 & e^{i\theta} (k_x - ik_y) \\ e^{-i\theta} (k_x + ik_y) & 0 \end{bmatrix} \psi'(\mathbf{k}).$$

Inter-layer coupling

- For each site in unrotated layer (layer 1) there is at most one site in the rotated layer (2) for which there is significant hopping:

$$\mathbf{r}'(\mathbf{r}) = \mathbf{r} + \delta(\mathbf{r}) \quad (\text{in-plane positions})$$

$$t_{\perp} \rightarrow t_{\perp}^{\alpha\beta}[\delta^{\alpha\beta}(r)] \equiv t_{\perp}^{\alpha\beta}(\mathbf{r}) \quad \alpha(\beta) = A, B(A', B')$$

$$\mathcal{H}_{\perp}^{(\mathbf{K})} = \sum_{\alpha, \beta} \sum_{\mathbf{k}, \mathbf{G}} \tilde{t}_{\perp}^{\alpha\beta}(\mathbf{G}) \psi_{\alpha, k + \Delta\mathbf{K}/2 + \mathbf{G}}^{\dagger} \psi_{\beta', k - \Delta\mathbf{K}/2} \quad (\Delta\mathbf{K} = \mathbf{K}^{\theta} - \mathbf{K})$$

$$\tilde{t}_{\perp}^{\alpha\beta}(\mathbf{G}) = \frac{1}{V_c} \int_{uc} d^2 r \, t_{\perp}^{\alpha\beta}(\mathbf{r}) e^{i\mathbf{K}^{\theta} \cdot \delta_{AB}(r)} e^{-i\mathbf{G} \cdot \mathbf{r}}$$

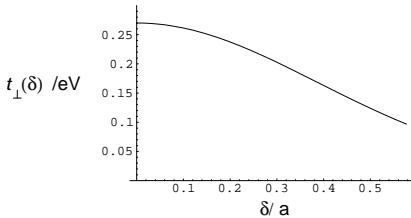
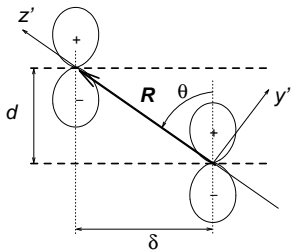
Full Hamiltonian

Choose \mathbf{k} origin at mid-point between Dirac points of the two layers.

$$\begin{aligned}\phi_{\alpha,k} &= \psi_{\alpha,k+\Delta K/2} && \text{in layer 1;} \\ \phi_{\alpha',k} &= \psi_{\alpha',k-\Delta K/2} && \text{in layer 2;}\end{aligned}$$

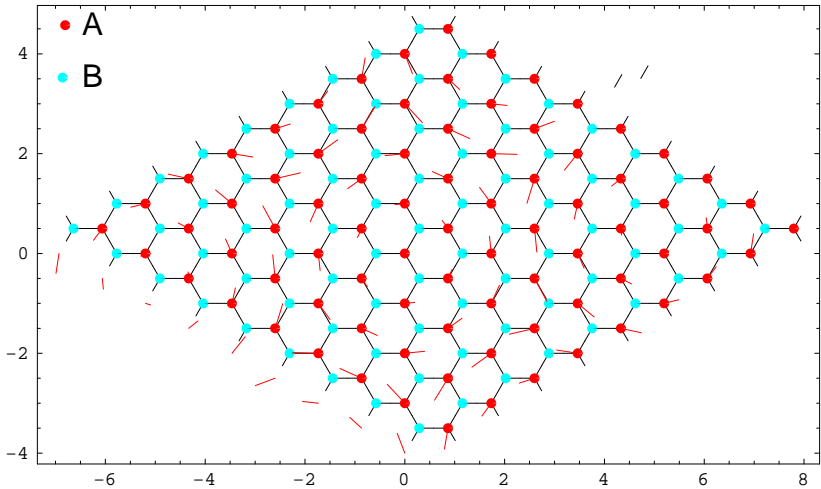
$$\begin{aligned}\mathcal{H} = & \hbar \sum_k \phi_{\alpha,k}^\dagger v_F \tau \cdot \left(\mathbf{k} + \frac{\Delta \mathbf{K}}{2} \right) \phi_{\beta,k} \\ & + \hbar \sum_k \phi_{\alpha',k}^\dagger v_F \tau^\theta \cdot \left(\mathbf{k} - \frac{\Delta \mathbf{K}}{2} \right) \phi_{\beta',k} \\ & + \sum_{\alpha,\beta} \sum_{\mathbf{k},\mathbf{G}} \tilde{t}_\perp^{\alpha\beta}(\mathbf{G}) \phi_{\alpha,k+G}^\dagger \phi_{\beta',k}.\end{aligned}$$

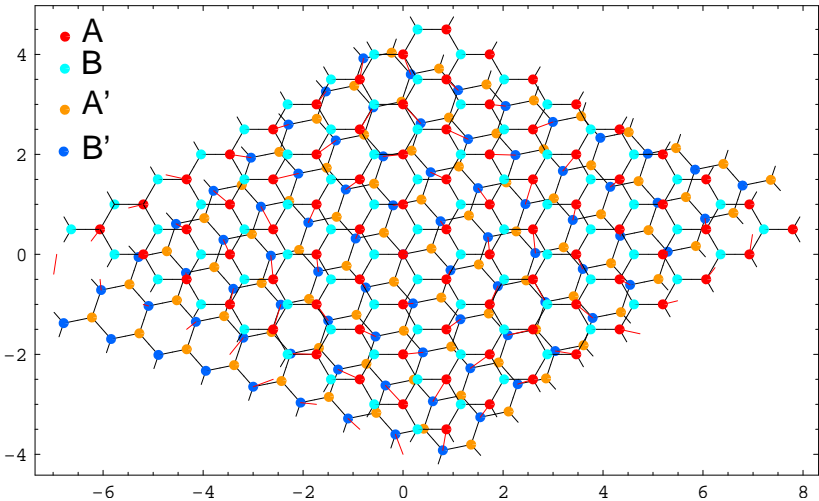
Calculation of $t_{\perp}(r)$



- $V_{pp\sigma}(r)$ and $V_{pp\pi}(r)$ can be estimated from values of $t \approx 2.78 \text{ eV}$, $t' \approx -0.12 \text{ eV}$ and $t_{\perp} \approx 0.27 \text{ eV}$.

Calculation of $\delta^{\alpha\beta}(\mathbf{r})$





Results for $\tilde{t}_\perp^{\alpha\beta}(\mathbf{G})$

\mathbf{G}	$\tilde{t}_\perp^{AB}(\mathbf{G})/$	$\tilde{t}_\perp^{AA}(\mathbf{G})$	$\tilde{t}_\perp^{BA}(\mathbf{G})$	$\tilde{t}_\perp^{BB}(\mathbf{G})$
(0, 0)	0.102	0.102	0.102	0.102
(0, 1)	0.014	0.014	0.014	0.014
(1, 1)	0.014	0.014	0.014	0.014
(2, 0)	0.004	0.004	0.004	0.004

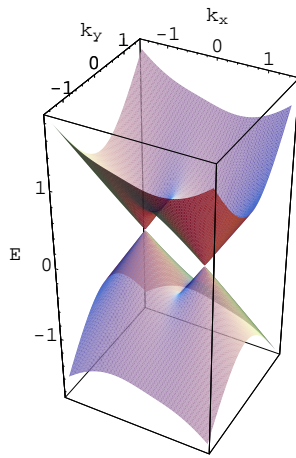
Values in eV. Absolute values, for $\mathbf{G} \neq 0$.

- Exact symmetries relate $\delta^{AB} \leftrightarrow \delta^{BA}$ and $\delta^{AA}, \delta^{AA} \leftrightarrow \delta^{BB}$.

Keeping $\tilde{t}_\perp^{\alpha\beta}(\mathbf{G} = 0)$

- New energy scale: $\hbar v_F \Delta K \approx 370 \text{ meV}$

$$\mathbf{H}(q) = \hbar v_F |\Delta K| \begin{bmatrix} 0 & q^* - \frac{1}{2} & Q_\perp & Q_\perp \\ q - \frac{1}{2} & 0 & Q_\perp & Q_\perp \\ Q_\perp & Q_\perp & 0 & e^{i\theta} (q^* + \frac{1}{2}) \\ Q_\perp & Q_\perp & e^{-i\theta} (q + \frac{1}{2}) & 0 \end{bmatrix}$$



- Full geometrical description of rotated layers (commensurability)
- Workable continuum description for slightly rotated layers: "quasi-free" Dirac electrons
- Preliminary results on electronic structure.